



Seminario PINNs

A Physics-informed Deep Neural Network for Harmonization of CT Images

- Mojtaba Zarei, Saman Sotoudeh Paima, Cindy McCabe, Ehsan Abadi, and Ehsan Samei -

Francisco de Izaguirre
Septiembre 2024



FACULTAD DE
INGENIERÍA



UNIVERSIDAD
DE LA REPÚBLICA
URUGUAY

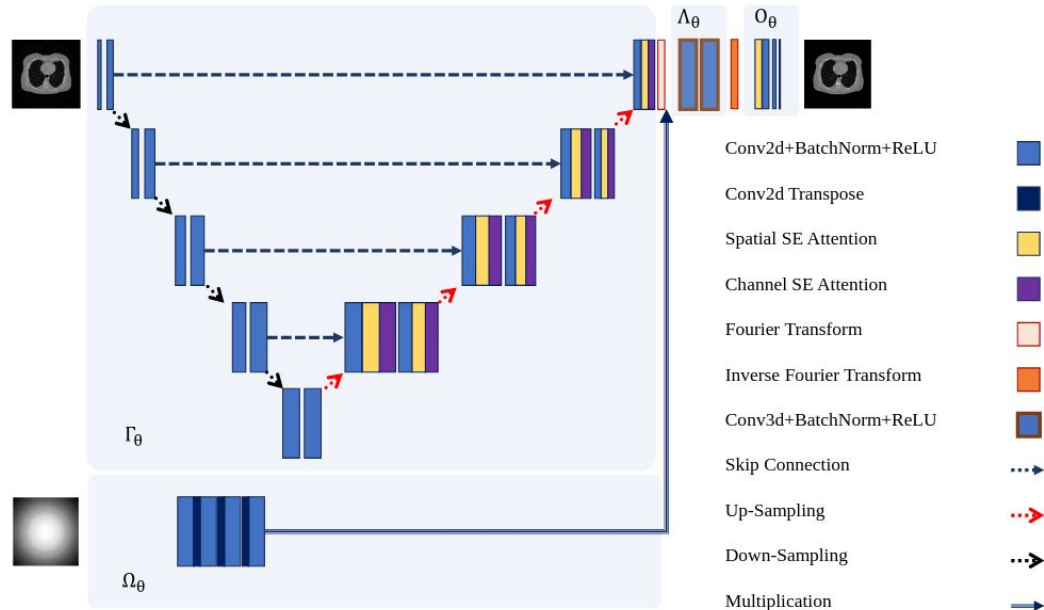


Índice

1. Disparador
2. Presentación del dominio de aplicación
 - a. Problema
 - b. Armonización de imágenes
3. Presentación de elementos
 - a. GANs
 - b. U-NET
 - c. “Squeeze and Excitation” Blocks
 - d. Elementos ópticos
4. Presentación de la arquitectura
5. Metodología
 - a. Dataset
 - b. Estimación de MTF
 - c. Losses
6. Repaso de lo propuesto
7. Resultados que obtienen

Disparador

Objective: Computed Tomography (CT) quantification is affected by the variability in image acquisition and rendition. This paper aimed to reduce this variability by harmonizing the images utilizing physics-based deep neural networks (DNNs). Methods: An adversarial generative network was trained on virtual CT images acquired under various imaging conditions using a virtual imaging platform with 40 computational patient models. These models featured anthropomorphic lungs with different levels of pulmonary diseases, including nodules and emphysema. Imaging was conducted using a validated CT simulator at two dose levels and varying reconstruction kernels. The trained model was tested on an independent virtual test dataset and two clinical datasets.





Presentación del dominio de aplicación

Procesamiento de tomografías computadas.

Problema:

Cambios en el dominio producidos por:

1. Adquisición de la imagen
 - a. Tomógrafo
 - b. Dosis de contraste
2. Reconstrucción de la imagen
3. Biología del paciente
4. Ruido asociado por el paciente

Presentación del dominio de aplicación

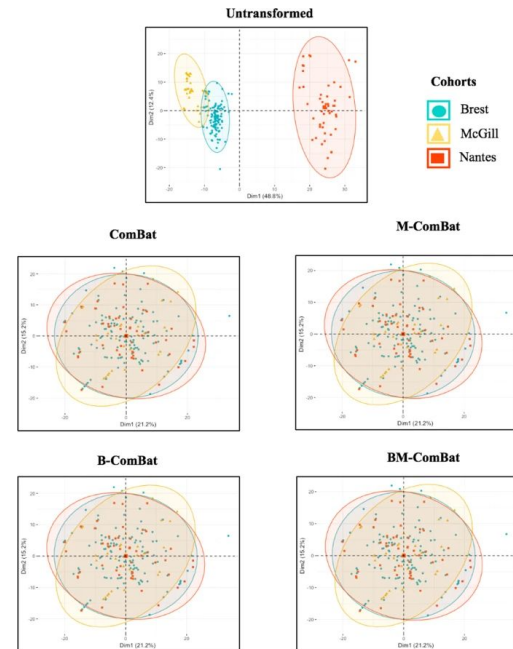
Armonización de imágenes

Definición: Encontrar invarianza en los dominios

Métodos clásicos:

1. Combat
2. Métodos basados en Bayes

“While these approaches are promising, they are influenced by their sensitivity to assumptions about the data distribution and linearity, batch size, data scaling, parameter initialization, and potential removal of true biological variability “



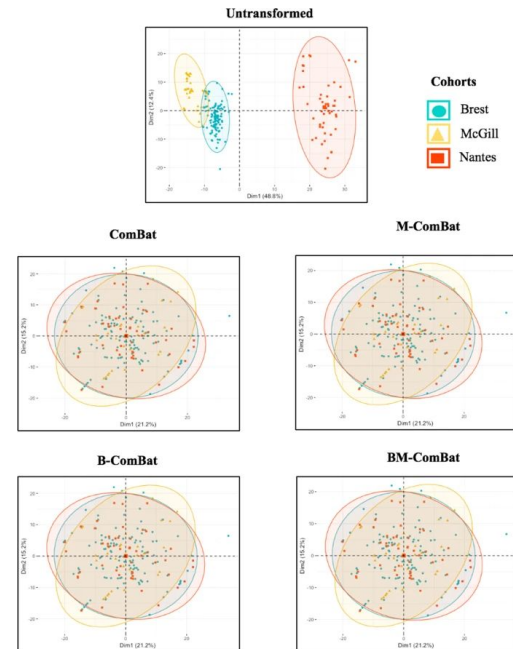
Presentación del dominio de aplicación

Armonización de imágenes

Definición: “Harmonization refers to minimizing the variance of image quantifications across datasets acquired using a variety of imaging protocols and scanner model”

Métodos clásicos:

1. Combat
2. Métodos basados en Bayes





Presentación de elementos

Generative Adversarial Network (GAN)

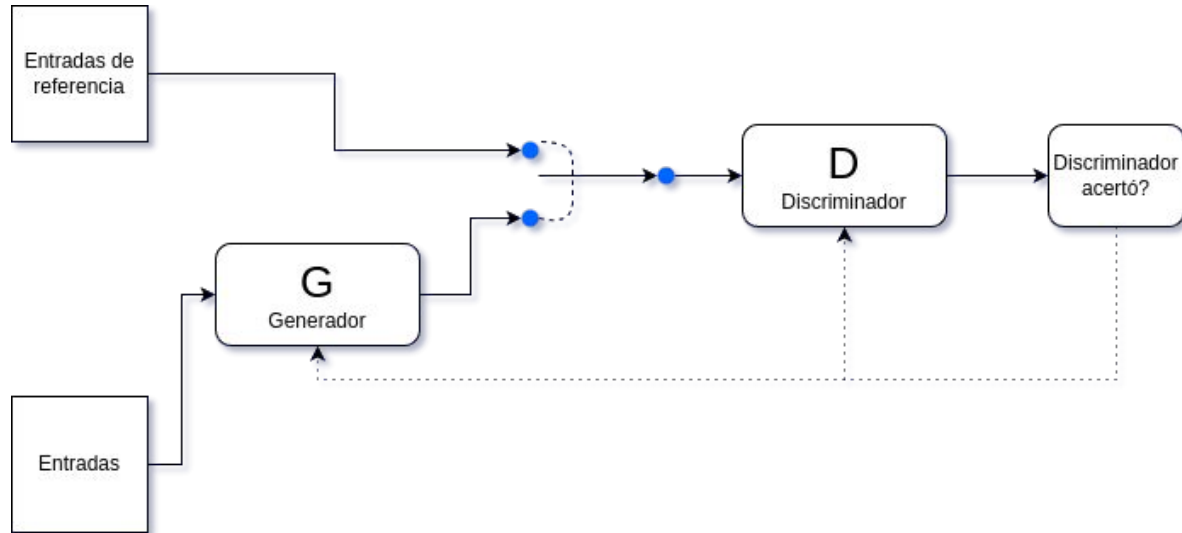
Porqué?

“..offer a methodology to align distributions and learn invariant features, and thus an opportunity for harmonizing medical images..”

“...in improving the reproducibility and performance of radiomic features in CT scans...”

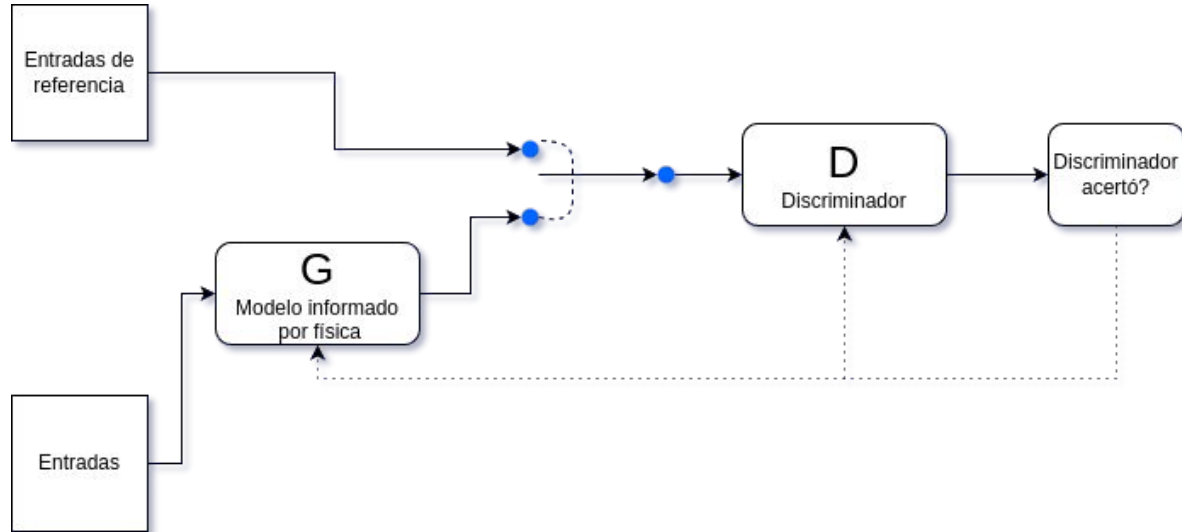
Presentación de elementos

Generative Adversarial Network (GAN)



Presentación de elementos

Generative Adversarial Network (GAN)



Presentación de elementos

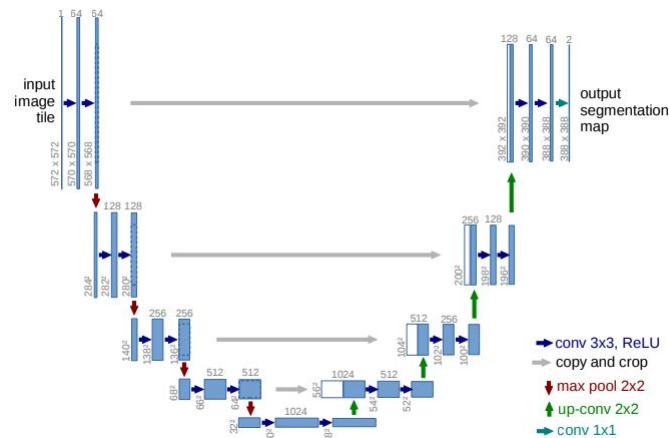
U-NET

Originalmente propuesta para segmentación de imágenes médicas

Es completamente convolucional.

El decoder logra mantener las estructuras y contexto que se observan en el encoder

“The architecture consists of a contracting path to capture context and a symmetric expanding path that enables precise localization”



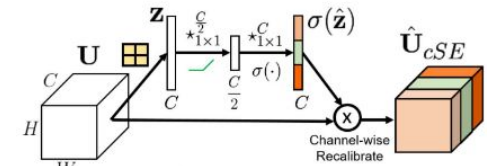
Presentación de elementos

“Squeeze and Excitation” Blocks

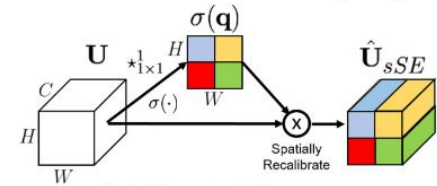
cSE - Priorizar canales importantes

sSE - Ayuda a una segmentación más fina

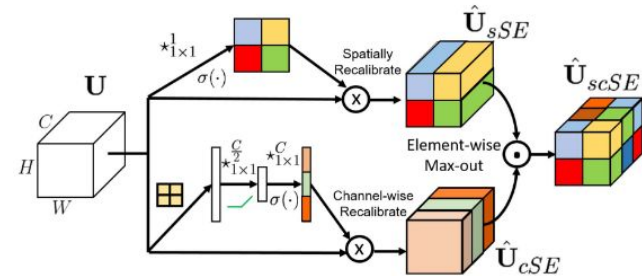
Mecanismos de atención



(a) Spatial Squeeze and Channel Excitation (cSE)



(b) Channel Squeeze and Spatial Excitation (sSE)



(c) Concurrent Spatial and Channel Squeeze and Channel Excitation (scSE)

$\star_{m \times n}^p$ Convolution with $m \times n$ kernel p channels
ReLU Global Pooling $\sigma(\cdot)$ Sigmoid

Presentación de elementos

Elementos ópticos

Point Spread Function (PSF) - Respuesta al impulso 2D

Module Transfer Function (MTF)

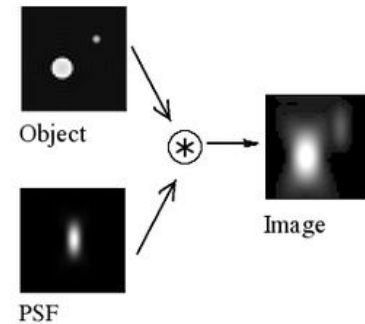
Optical Transfer Function (OTF)

Edge Spread Function (ESF) - Respuesta a un borde

Lineal Spread Function (LSF) - Respuesta de un borde infinitesimal

Resolution Index (RI)

Isocentro - Punto del espacio sobre el que gira la unidad



Presentación de elementos

Elementos ópticos

Point Spread Function (PSF) - Respuesta al impulso 2D

Module Transfer Function (MTF)

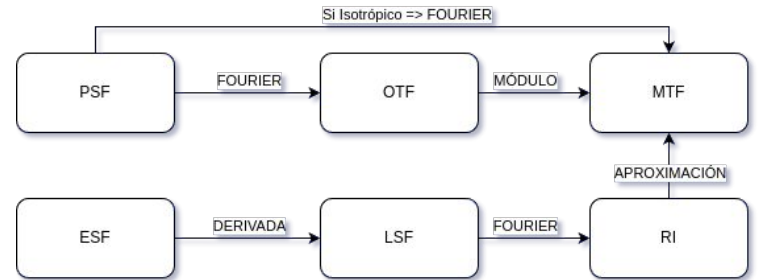
Optical Transfer Function (OTF)

Edge Spread Function (ESF) - Respuesta a un borde

Lineal Spread Function (LSF) - Respuesta de un borde infinitesimal

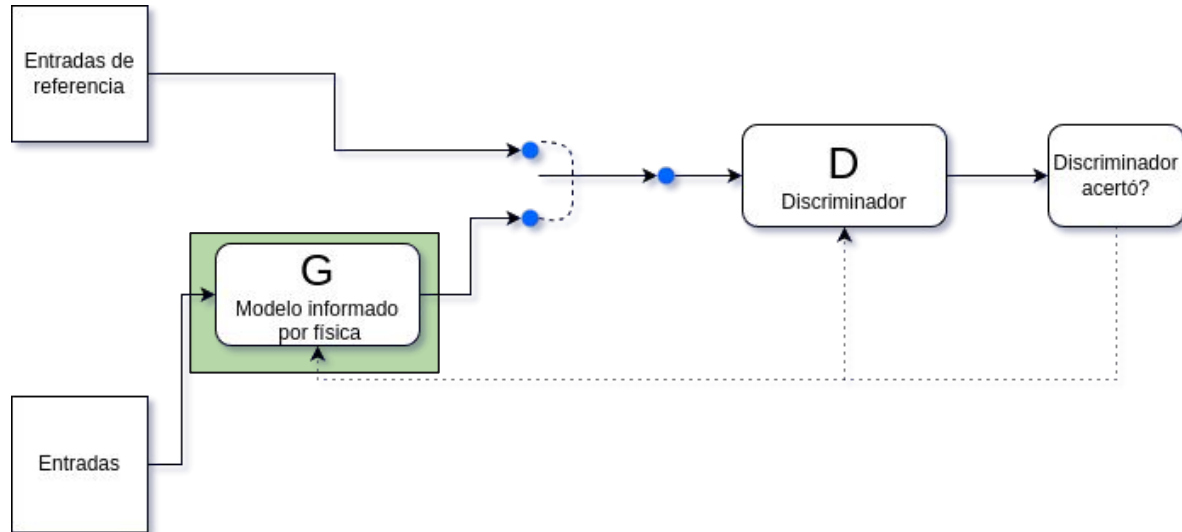
Resolution Index (RI)

Isocentro - Punto del espacio sobre el que gira la unidad

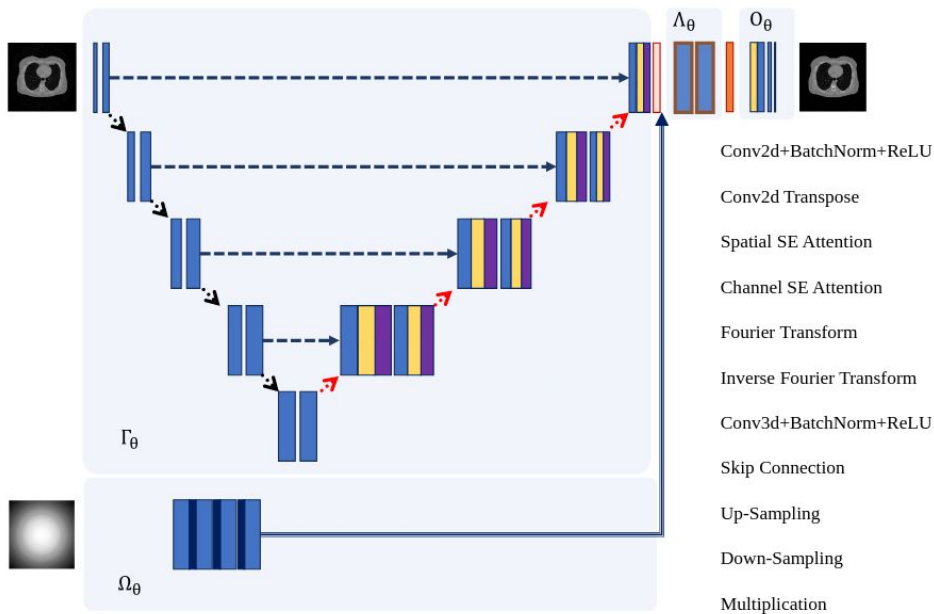


Presentación de elementos

Generative Adversarial Network (GAN)



Presentación de la arquitectura



$$I_b(x, y) = \mathcal{F}^{-1} \left[\mathcal{F}[I_a(x, y)] \times \frac{\mathcal{F}[PSF_b(x, y)]}{\mathcal{F}[PSF_a(x, y)]} \right], \quad (1)$$

$$I_b(x, y) = \mathcal{F}^{-1} \left[\mathcal{F}[I_a(x, y)] \times MTF_{ratio}(w) \right]. \quad (2)$$

$$I_h(x, y) = O_\theta \left(\mathcal{F}^{-1} \left[\Lambda_\theta \left(\mathcal{F}[\Gamma_\theta(I_{nh}(x, y))], \Omega_\theta(MTF_{2D}) \right) \right] \right) = G_\theta(I_{nh}(x, y), MTF_{2D}), \quad (3)$$



Metodología

Dataset

40 XCAT simulados.

32 versiones (variación de kernels y de dosis)

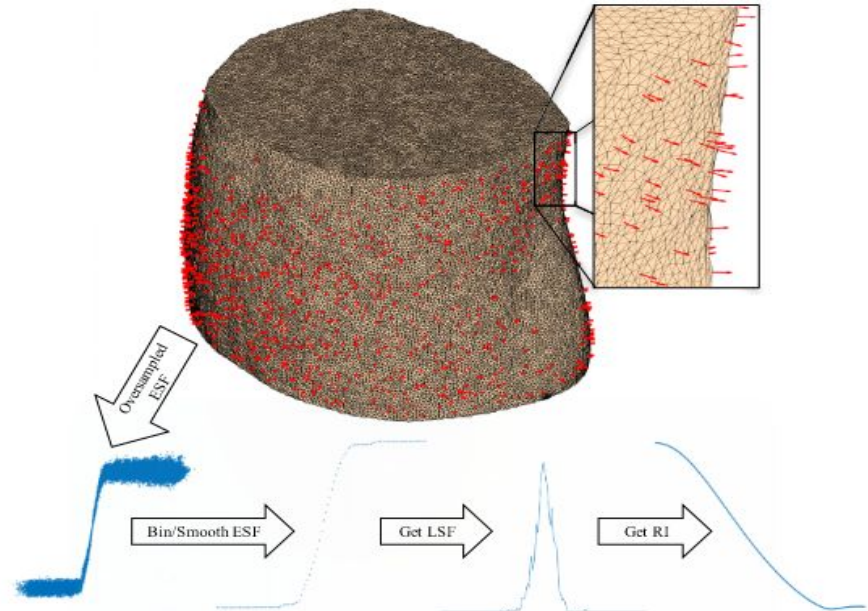
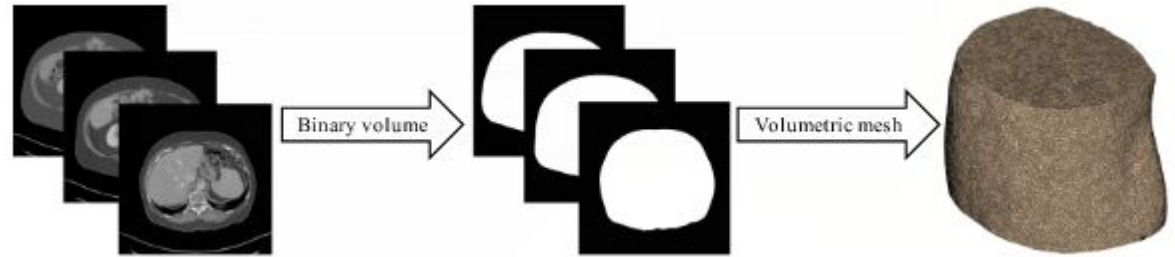
Dataset con imágenes reales para testing



Metodología

Estimación de MTF

- 1 - Se segmenta el cuerpo
- 2 - Se estima la ESF en la interfaz aire-piel
- 3 - Se estima la MTF





Metodología

Losses

1 - Hubber (distancia pixeles)

2 - Wasserstein con penalización de gradiente (adversaria)

3 - Perceptual (textura)

$$\mathcal{L}_d(I_h, I_r) = \begin{cases} 0.5 \cdot (I_h - I_r)^2, & \text{if } |I_h - I_r| \leq \delta \\ \delta \cdot (|I_h - I_r| - 0.5 \cdot \delta), & \text{if } |I_h - I_r| > \delta \end{cases}, \quad (4)$$

$$\text{WGAN}_{\text{GP}} = D_{\theta}(I_{r,nh}) - \mathbb{E}[D_{\theta}(I_{h,nh})] + \lambda_{\text{GP}} \mathbb{E}[(\|\nabla_{\tilde{I}} D_{\theta}(\tilde{I})\|_2 - 1)^2], \quad (5)$$

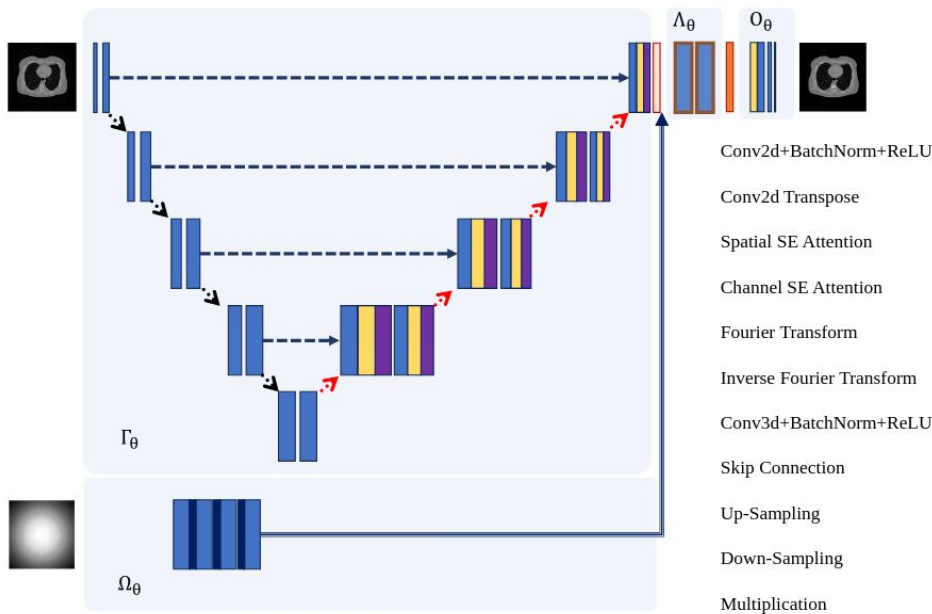
$$\mathcal{L}_a(I_h) = \mathbb{E}[D_{\theta}(I_{h,nh})]. \quad (6)$$

$$\mathcal{L}_t(I_h, I_r) = \sum_{i=1}^N \text{MSE} \left(\frac{Gm(\text{VGG}_i(I_h))}{\|Gm(\text{VGG}_i(I_h))\|}, \frac{Gm(\text{VGG}_i(I_r))}{\|Gm(\text{VGG}_i(I_r))\|} \right), \quad (7)$$

$$\mathcal{L}_H(I_h, I_r) = \lambda_d \mathcal{L}_d(I_h, I_r) + \lambda_a \mathcal{L}_a(I_h) + \lambda_t \mathcal{L}_t(I_h, I_r), \quad (8)$$

$$\lambda_d = 1000, \lambda_t = 50, \text{ and } \lambda_a = 1$$

Repaso de lo propuesto

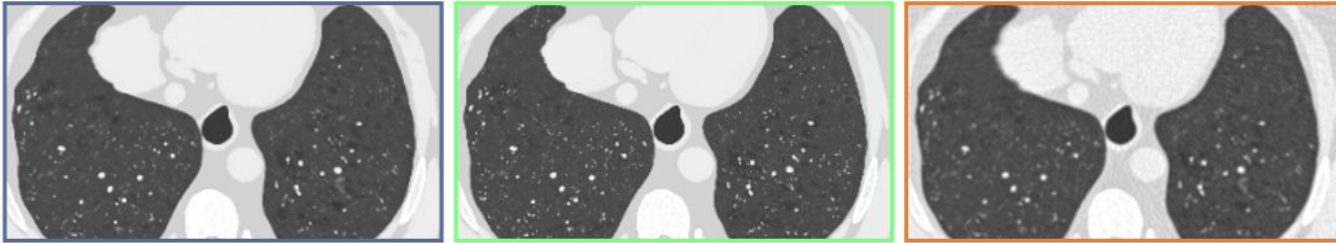


$$I_b(x, y) = \mathcal{F}^{-1} \left[\mathcal{F}[I_a(x, y)] \times \frac{\mathcal{F}[PSF_b(x, y)]}{\mathcal{F}[PSF_a(x, y)]} \right], \quad (1)$$

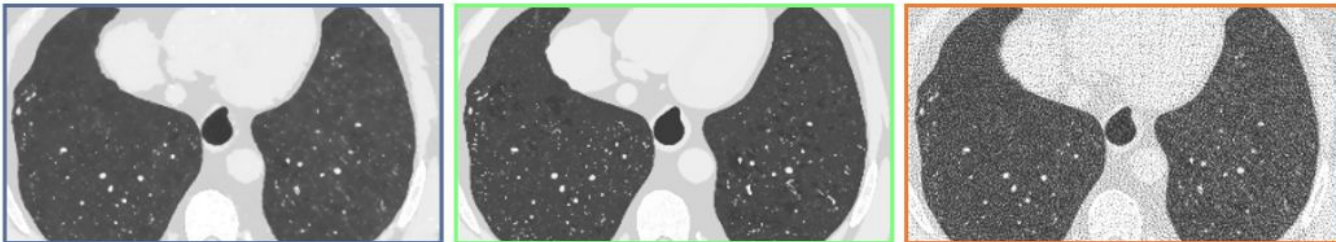
$$I_b(x, y) = \mathcal{F}^{-1} \left[\mathcal{F}[I_a(x, y)] \times MTF_{ratio}(w) \right]. \quad (2)$$

$$I_h(x, y) = O_\theta \left(\mathcal{F}^{-1} \left[\Lambda_\theta \left(\mathcal{F}[\Gamma_\theta(I_{nh}(x, y))], \Omega_\theta(MTF_{2D}) \right) \right] \right) = G_\theta(I_{nh}(x, y), MTF_{2D}), \quad (3)$$

Resultados que obtienen



(a) High dose and smooth kernel rendition.



(b) Low dose and sharp kernel rendition.

Resultados que obtienen

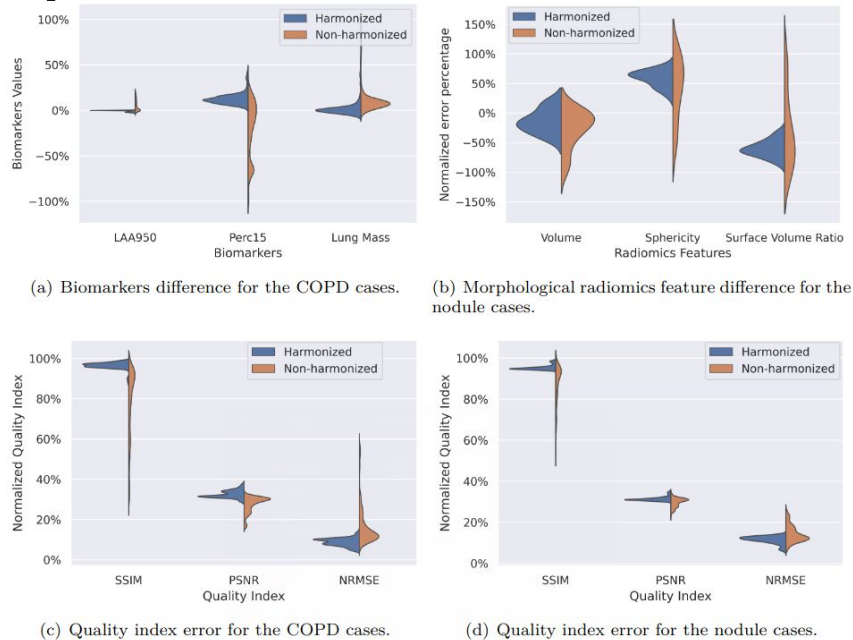


Fig. 3. The quantitative outcomes for the nodule cases (right column) and COPD cases (left column). To compare the PSNR values with other measurements, their values in dB were divided by 100.

Resultados que obtienen

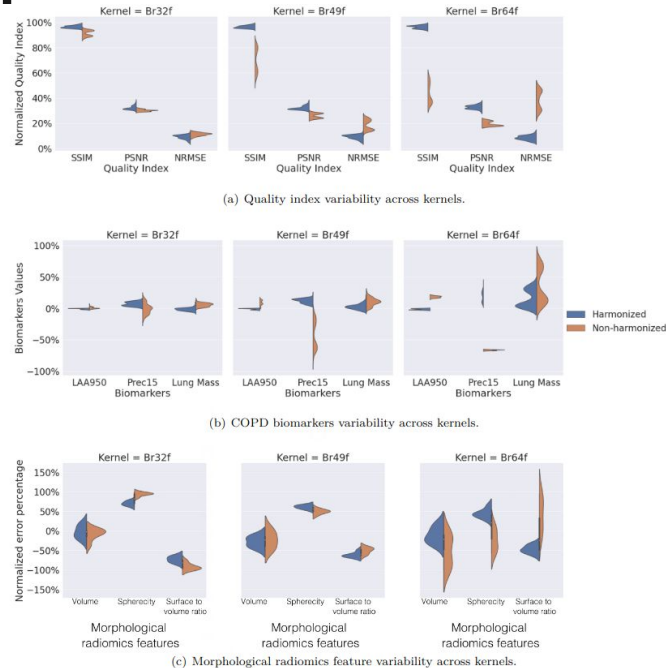


Fig. 4. Analyzing the differences in bias and variability between harmonized and non-harmonized images according to the deployed smooth, average, and sharp kernels.

Resultados que obtienen

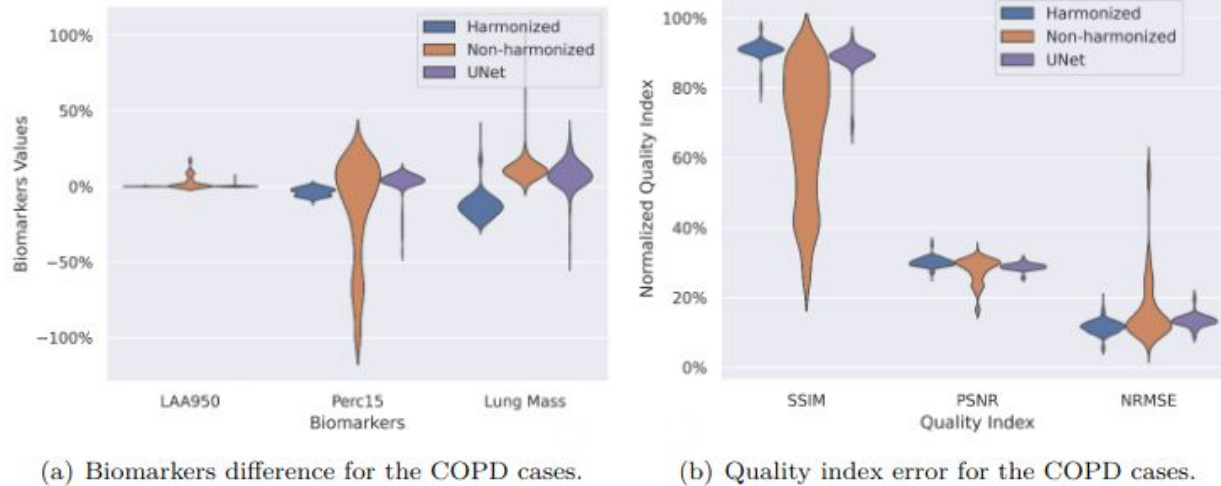
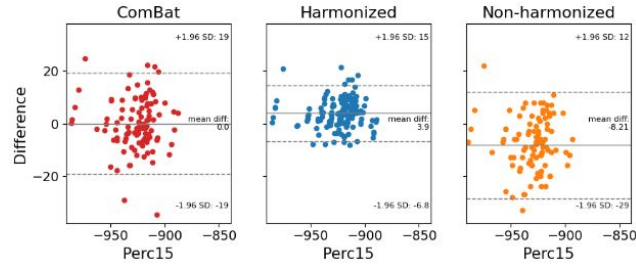
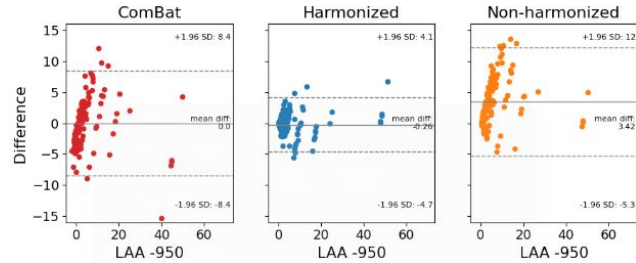


Fig. 5. The quantitative outcomes for COPD cases in the ablation study. To compare the PSNR values with other measurements, their values in dB were divided by 100. The blue, red, and purple data are measured metrics and biomarkers from the harmonized, non-harmonized, and Unet output images, respectively.

Resultados que obtienen



(a) Perc 15 variability.



(b) LAA -950 variability.

Fig. 6. COPD biomarkers variability and bias with respect to the smooth kernel and high dose renditions in COPDGene dataset. The results, from left to right, were obtained from the ComBat feature harmonization algorithm, proposed harmonizer, and non-harmonized images, respectively.

Resultados que obtienen

TABLE II

QUANTITATIVE RESULTS ON THE TEST SET WITH LUNG NODULE INSERTED. THE FIRST THREE METRICS WERE MEASURED ON A SINGLE 2D SLICE, AND RADIOMICS FEATURES WERE MEASURED ON THE 3D SLICES.

	NRMSE (%)	SSIM (%)	PSNR (dB)
H	11.5±1.9	95.1±1.3	31.3±1.1
NH	14.2±4.0	87.4±9.1	29.6±2.3
	$V_{\text{NRMSE}}(\%)$	$A/V_{\text{NRMSE}}(\%)$	$S_{\text{NRMSE}}(\%)$
H	2.1±1.3	14.2±3.0	16.5±3.8
NH	3.4±2.5	14.8±6.9	16.3±8.45

TABLE III

QUANTITATIVE RESULTS ON THE COPD TEST SET FOR THE ABLATION STUDY. ALL METRICS WERE MEASURED ON A SINGLE 2D SLICE.

	NRMSE (%)	SSIM (%)	PSNR (dB)
H	11.5±1.9	91.0±2.5	30.2±1.4
UNet	13.4±1.9	88.4±4.2	28.8±1.0
	$ \Delta _{\text{LAA -950}}(\%)$	$ \Delta _{\text{Perc 15}}(\text{HU})$	$ \Delta _{\text{Lung mass}}(\text{g})$
H	0.17±0.24	6.3±4.1	0.3±0.12
UNet	0.54±1.93	10.7±10.9	0.1±0.07

TABLE IV

VARIABILITY ANALYSIS IN QUANTIFICATION OF THE COPD BIOMARKERS FOR HARMONIZED AND NON-HARMONIZED IMAGES.

	Kernel	Dose	LAA -950	Perc 15
H	-	-	1.11	-915
NH	Smooth	Regular	1.91	-922
H	-	-	5.17	-932
NH	Medium	Regular	11.81	-946
H	-	-	3.87	-919
NH	Smooth	Low	7.86	-931
H	-	-	1.83	-920
NH	Smooth	Low	6.19	-932
H	-	-	1.86	-915
NH	Smooth	Low	2.54	-923

Resultados que obtienen

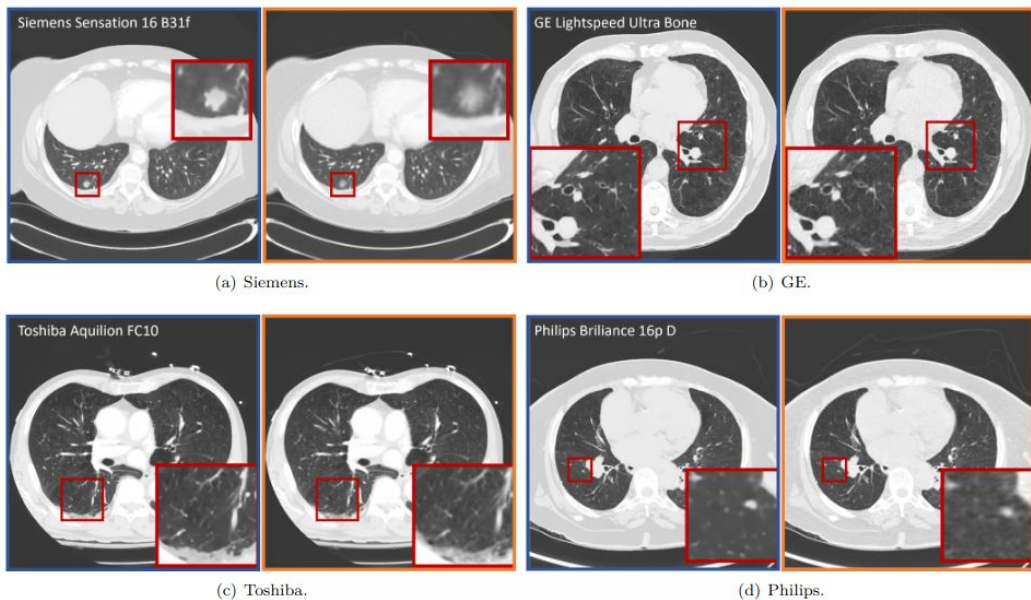


Fig. 9. Harmonization results across different vendors. Non-harmonized (in orange square) and the corresponding harmonized (in blue square) images.